The Journal of Immunology

RESEARCH ARTICLE | APRIL 15 2010

Characterization of Synergistic Induction of CX3CL1/Fractalkine by TNF-α and IFN-γ in Vascular Endothelial Cells: An Essential Role for TNF-α in Post-Transcriptional Regulation of CX3CL1 FREE

Tomoh Matsumiya; ... et. al

J Immunol (2010) 184 (8): 4205–4214.
https://doi.org/10.4049/jimmunol.0903212

Characterization of Synergistic Induction of CX3CL1/Fractalkine by TNF-α and IFN-γ in Vascular Endothelial Cells: An Essential Role for TNF-α in Post-Transcriptional Regulation of CX3CL1

Tomoh Matsumiya,* Ken Ota,† Tadaatsu Imaizumi,* Hidemi Yoshida,* Hiroto Kimura,‡ and Kei Satoh*

CX3CL1/Fractalkine, a chemokine specific to monocytes and NK cells, is induced synergistically by TNF-α and IFN-γ in vascular endothelial cells. However, the mechanism for this synergism remains unclear. This study explored the hypothesis that the CX3CL1 expression is regulated at a posttranscriptional level, which may responsible for the synergism between TNF-α and IFN-γ. Brief exposure of HUVECs to TNF-α led to a robust increase in IFN-γ–induced CX3CL1 production. We found that TNF-α stabilized CX3CL1 mRNA in HUVECs stimulated with IFN-γ. Cloning of 3′untranslated region (UTR) of CX3CL1 mRNA revealed the presence of a single copy of nonametric AU-rich element in its 3′UTR, and a luciferase reporter assay showed that a single AU-rich element is a crucial *cis*-element in the posttranscriptional regulation of CX3CL1. TNF-α treatment resulted in the phosphorylation of p38 MAPK and its downstream target, MAPK-activated protein kinase-2, but IFN-γ did not affect the levels of MAPK and MAPK-activated protein kinase-2 phosphorylation induced by TNF-α. Treatment of the cells with an inhibitor of p38 MAPK accelerated the decay of CX3CL1 mRNA induced by TNF-α or the combination of TNF-α and IFN-γ. Immunoprecipitation assay revealed that mRNA stabilizer HuR directly binds to 3′UTR of CX3CL1 mRNA. CX3CL1 expression is under control of posttranscriptional regulation, which is involved in the synergistic induction of CX3CL1 in response to the combined stimulation with TNF-α and IFN-γ. *The Journal of Immunology*, 2010, 184: 4205–4214.

Infiltration and accumulation of monocytes/macrophages into the subendothelial space are prominent pathologic features of atherosclerosis (1). However, the mechanisms for monocyte recruitment and infiltration are not fully understood. Recent studies revealed the high levels of cytokine expression in the region of the atheroma compared with normal arteries (2). TNF-α and IFN-γ, major proinflammatory cytokines, are detected at particularly high levels as compared with anti-inflammatory cytokines (e.g., IL-4, IL-10) (3). TNF-α, a pleiotropic cytokine that exerts potent proinflammatory effects, is implicated in atherosclerosis and other metabolic and inflammatory disorders, such as obesity and insulin resistance (4). The major source of TNF-α is monocytes/macrophages (5). IFN-γ is secreted mainly by NK cells and activated T lymphocytes (CD4+ Th1 cells) (6). Th1 cells, regarded as proatherogenic, accumulate in the plaques with enhanced expression of IFN-γ (7). IFN-γ has a wide variety of functions, including antiviral, immunomodulatory, and inflammatory activities (6). Both TNF-α and IFN-γ serve as agonists to induce a variety of cytokines, and costimulation of cells with TNF-α and IFN-γ leads to synergistic superinduction of a certain type of cytokines (8).

CX3CL1, also known as fractalkine, is a unique chemokine categorized to the CX3CL1 chemokine family (9). CX3CL1 has potent chemoattractant activity for T cells and monocytes, along with MCP-1 known as CCL2 (10). A recent animal study demonstrated the resistance to development of atherosclerosis in *cx3cl1*$^{-/-}$ *apoE*$^{-/-}$ mice or *cx3cl1*$^{-/-}$*ldlr*$^{-/-}$ mice, suggesting that CX3CL1 plays an important role in the plaque formation by recruiting monocytes/macrophages (11). The expression of CX3CL1 is enhanced synergistically by TNF-α and IFN-γ (12–15). The individual effect of either TNF-α or IFN-γ is limited to induce CX3CL1; however, the combined treatment of HUVECs with these cytokines increases the CX3CL1 protein levels ~10-fold (12). Therefore, the elucidation of the molecular mechanisms underlying this synergistic effect may provide an important insight into pathogenesis of atherosclerosis.

In the fields of immunology and virology, it has been known that simultaneous treatment with TNF-α and IFN-γ synergistically induces the antiviral responses, which inhibits viral gene expression and lower viral titers to a greater extent than those brought about by the treatment with either one of these cytokines (16). TNF-α activates NF-κB (NF-κB) (17). IFN-γ activates JAK and its subsequent downstream molecule, STAT1 (18). Functional synergy between TNF-α and IFN-γ is thought to be mediated by signal cross-talk between the JAK–STAT pathway and NF-κB system (19, 20). Moreover, many of the genes, under the synergistic regulation by

*Department of Vascular Biology, Institute of Brain Science, †Department of Gastroenterology and Hematology, and ‡Department of Oral and Maxillofacial Surgery, Hirosaki University Graduate School of Medicine, Hirosaki, Japan

Received for publication October 1, 2009. Accepted for publication February 5, 2010.

This work was supported in part by a Grant-in-Aid for Scientific Research (KAKENHI) (20591934 to T.M.), the Fund for the Promotion of International Scientific Research (to T.M.), and The Karoji Memorial Fund for Medical Research (to T.M.).

The sequences presented in this article have been submitted to GenBank (www.ncbi.nlm.nih.gov/Genbank/) under accession number GU047346.

Address correspondence and reprint requests to Dr. Tomoh Matsumiya, Department of Vascular Biology, Institute of Brain Science, Hirosaki University Graduate School of Medicine, 5 Zaifu-cho, Hirosaki City, Aomori 036-8562, Japan. E-mail address: tomo1027@cc.hirosaki-u.ac.jp

Abbreviations used in this paper: Act D, actinomycin D; ARE, AU-rich element; IP, immunoprecipitated; MAPKAPK, MAPK-activated protein kinase; pcDNA and pCMV-HA, plasmid cDNA; Sup, supernatant; UTR, untranslated region.

TNF-α and IFN-γ, including *ICAM1* (21), *IRF1* (22), and *CX3CL1* (15), have the DNA binding *cis*-elements for both STAT1 and NF-κB within their promoter regions.

It is, however, not yet fully understood how TNF-α and IFN-γ synergistically induce gene expression, because TNF-α has the ability to regulate gene expression at both the transcriptional and posttranscriptional levels (23). Surprisingly, no studies to date have investigated the role of the posttranscriptional gene regulation by TNF-α in the synergism with IFN-γ. The present study was undertaken to examine the potential involvement of post-transcriptional regulation of CX3CL1 mRNA induced by TNF-α and IFN-γ in cultured human endothelial cells.

Materials and Methods

Cell culture

HUVECs (Lonza, Basel, Switzerland) were cultured as described previously (24) with slight modification. The cells were maintained in a 5% CO_2 atmosphere at 37˚C in endothelial growth medium containing supplements (FBS [2%], hydrocortisone [0.04%], ascorbic acid [0.1%], long R insulin-like growth factor-1 [0.1%], heparin [0.1%], human fibroblast growth factor [0.4%], human recombinant vascular endothelial growth factor [0.1%], human recombinant epidermal growth factor [0.1%], and gentamicin sulfate/amphotericin B [0.1%]). When the cells reached ~80% confluence, the medium containing growth factors was replaced with M-199 (Invitrogen, Carlsbad, CA) supplemented with 20% human serum. A549 cells were maintained in a 5% CO_2 atmosphere at 37˚C in DMEM (Invitrogen) supplemented with 10% FBS (Invitrogen). HUVECs were stimulated with 2 ng/ml TNF-α (R&D Systems, Minneapolis, MN) or 2 ng/ml IFN-γ (R&D Systems). Inhibition of p38 MAPK was accomplished by treating the cells with 1 μM SB203580 (Calbiochem, La Jolla, CA), a p38-specific inhibitor, for the indicated time periods.

ELISA for CX3CL1

For the measurement of CX3CL1 production by HUVECs, the cells in a six-well culture plate were stimulated with 2 ng/ml IFN-γ for 16 h, followed by 2 ng/ml TNF-α treatment for up to 2 h. After the incubation, the cells were washed twice with M-199, and culture medium was replaced with M-199–0.5% BSA (Sigma-Aldrich, St. Louis, MO), and the cultures were incubated for an additional 90 min. Next, the conditioned medium was collected, cell debris was pelleted by centrifugation, and the level of CX3CL1 in the supernatant (Sup) was determined using a Quantikine ELISA kit (R&D Systems).

Quantitative RT-PCR

Total RNA was extracted from the cells using an RNeasy Total RNA Isolation kit (Qiagen, Hilden, Germany) with on-column DNase I (Qiagen) digestion. One microgram of total RNA served as a template for single-strand cDNA synthesis in a reaction using oligo(dT) primers and M-Mulv reverse transcriptase (Invitrogen) under conditions indicated by the manufacturer. An Opticon 2 real-time PCR detection system (Bio-Rad, Hercules, CA) was used for quantitative analyses of CX3CL1, GAPDH, luciferase, and zeocin. The sequences of the primers were as follows: CX3CL1-F (5′-GACCCCTAAGGCTGAGGAAC-3′), CX3CL1-R (5′-CTCTCCTGCCATCTTTCGAG-3′), GAPDH-F (5′-CCACCCATGGCAAATTCCATGGCA-3′), GAPDH-R (5′-TCTAGACGGCAGGTCAGGTCCACC-3′), Luciferase-F (5′-ACGGATTACCAGGGATTTCAGTC-3′), Luciferase-R (5′-AGGCTCCTCAGAAACAGCTCTTC-3′), Zeocin-F (5′-GACTTCGTGGAGGACGACTT-3′), and Zeocin-R (5′-GACACGACCTCCGACCACT-3′).The amplification reactions were performed with iQ SYBR Green Supermix (Bio-Rad) according to the manufacturer's specifications. Amplification conditions were as follows: 2 min at 50˚C followed by 3 min at 95˚C and then 40 cycles of 15 s at 95˚C, 30 s at 58˚C, and 30 s at 72˚C. After amplification was complete, a melting curve was generated by heating slowly at 0.1˚C per second to 95˚C with continuous collection of fluorescence. Melting curves and quantitative analysis of the data were performed using an Opticon monitor, version 3.1, as reported previously (25).

Polysome profile analysis

HUVECs grown in a 2 × 100-mm dish were treated with 100 μg/ml cycloheximide (Sigma-Aldrich) for 15 min, washed twice with ice-cold PBS (pH 7.4), and harvested in hypotonic lysis buffer (10 mM Tris [pH 7.4], 100 mM NaCl 1.5 mM $MgCl_2$, 0.5% NP-40) containing 0.2% protease inhibitor mixture and 100 U/ml RNase Out (Invitrogen). The mixtures were homogenized with the aid of a Dounce homogenizer and then subjected to centrifugation at 12,000 × *g* for 10 min at 4˚C. The supernatants were layered on a 15–45% sucrose gradient containing 10 mM Tris (pH 7.4), 100 mM NaCl, 1.5 mM $MgCl_2$, 10 μg/ml cycloheximide and 40 U/ml RNase Out and centrifuged at 30,000 rpm for 90 min at 4˚C in a Hitachi RPS40T rotor. The position of monosomes and polysomes was monitored by UV absorption at 254 nm. Eighteen fractions were collected from the bottom to the top of the centrifuge tubes, and the RNA from each gradient fraction (250 μl) was extracted by Trizol LS (Invitrogen). Aliquots were analyzed on a 1% agarose gel to resolve the polysome profile. CX3CL1 mRNA levels in each fraction were determined by real-time PCR as described above.

Cloning of the 3′ untranslated region for CX3CL1 *gene*

Cloning of CX3CL1 3′untranslated region (UTR) was performed by 3′ RACE using a 3′-Full RACE Core Set (Takara Biotechnology, Kusatsu, Japan). One microgram of total RNA from HUVECs treated with IFN-γ (2 ng/ml, 16 h) was used as a template. The oligo(dT)-3 sites adaptor was used for the synthesis of first strand cDNA by incubation with AMV reverse transcriptase and the total RNA for 1 h at 50˚C. The 3′UTR of CX3CL1 was amplified by PCR using Takara LA Taq (Takara Biotechnology), with the gene-specific primer, CX3CL1-GSP1 (5′-ATGTTCACCTACCAGAGCCTC-3′), and the 3′-sites adaptor primer (5′-CTGATCTAGAGGTACCGGATCC-3′) provided in the kit. Nested PCR was performed with the primers CX3CL1-GSP2 (5′-ACTCCTCTGGCCTGTGTCTAG-3′). Both of the PCR conditions were as follows: 1 cycle at 95˚C for 2 min; 30 cycles at 95˚C for 30 s, 50˚C for 30 s, and 72˚C for 1 min; and 1 cycle at 72˚C for 7 min. The amplified products were purified, inserted into a pTac-1 vector (BioDynamics Laboratory, Tokyo, Japan) and sequenced. The gene sequence has been submitted to GenBank.

Plasmid construction

Luciferase reporter expression constructs illustrated in Fig. 4*A* were prepared in the vector pcDNA3.1/Zeo(+) containing the firefly luciferase cDNA from pGL3-Basic (Promega, Madison, WI) cloned into the HindIII and XbaI sites to yield plasmid cDNA (pcDNA)-Luc as reported by Dixon et al. (26). Addition of the CX3CL1 3′UTR was accomplished by PCR amplifying the full-length CX3CL1-3′UTR using Phusion DNA polymerase (Finnzymes, Keilaranta, Finland) and XbaI-tailed primers, Xba-CX3CL1-3′UTR-F (5′-CGATCTAGAACTCCTCTGGCCTGTGTCTAG-3′), and Xba-CX3CL1-3′UTR-R (5′-GCTTCTAGACACAAGACTTTTAAATTTTATTAG-3′), to yield pcDNA-Luc-FL-UTR. The constructs pcDNA-Luc-UTR-ARE and pcDNA-Luc-UTR-ΔARE were prepared similarly as pcDNA-Luc-FL-UTR with the primers Xba-CX3CL1-3′UTR-F and Xba-UTR ARE-R (5′-GCTctagaTAGTACTCACAGGGCAGC-3′; for pcDNA-Luc-UTR-ARE), or Xba-CX3CL1-3′UTR-F and Xba-UTR-ΔARE-R (5′-GCTctagaGTTCATTGGGGCTGGGAT-3′; for pcDNA-Luc-UTR-ΔARE), respectively. A point mutation in ARE was generated using a site-directed mutagenesis kit (Stratagene, La Jolla, CA). CX3CL1 3′UTR full-length and UTR-ARE cDNA were cut out, using XbaI, from pcDNA-Luc-FL-UTR and pcDNA-Luc-UTR-ARE, respectively. After the purification, each of these cDNAs was inserted into the XbaI site of pBluescript SKII (+) (Stratagene). Supercoiled dsDNA vectors containing the insert of interest were amplified using two complementary oligonucleotide primers containing U > G mutation in the center of ARE nonamer. After amplification, the parental DNA encoding CX3CL1 3′UTR or UTR-ARE containing wild type ARE was digested with DpnI to select formulation-containing synthesized DNA. The primer sequences and their complement were 5′-CAATGAACAATTATGTATTAAATGCCCAG-3′ and 5′-CTGGGCATTTAATACATAATTGTTCATTG-3′. To construct a clone lacking ARE nonamer from the full-length CX3CL1 3′UTR or UTR-ARE, pBluescript SKII(+)-FL-UTR or -UTR-ARE was amplified by an inverted PCR method using *Pfu* Turbo DNA polymerase (Stratagene) with a primer set of deletion-F (5′-AAATGCCCAGCCCCTTCTGAC-3′) and deletion-R (5′-TTGTTCATTGGGGCTGGGAT-3′). PCR product was purified, treated with T4 kinase (Fermentas, Glen Burnie, MD) and then self-ligated using T4 ligase (Fermentas). After confirming the mutations by DNA sequencing, the mutated cDNA was cut with XbaI from each of the pBluescript SKII(+) vectors and inserted into the XbaI site of pcDNA-Luc vector again. cDNA encoding full-length HuR was amplified using cDNA isolated from HeLa cells with Phusion DNA polymerase and the primers, EcoRI-HuR-F (5′-AGGAATTCCCATGTCTAATGGTTATGAAGAC-3′) and NotI-HuR-R (5′-TATGCGGCCGCTTATTTGTGGGACTTGTTGG-3′). The amplified product was inserted into the EcoRI and NotI sites of a mammalian expression vector, pCMV-HA (Clontech, Palo Alto, CA). All DNA constructs were analyzed by DNA sequencing. Plasmid DNAs were purified using a plasmid purification column (Qiagen).

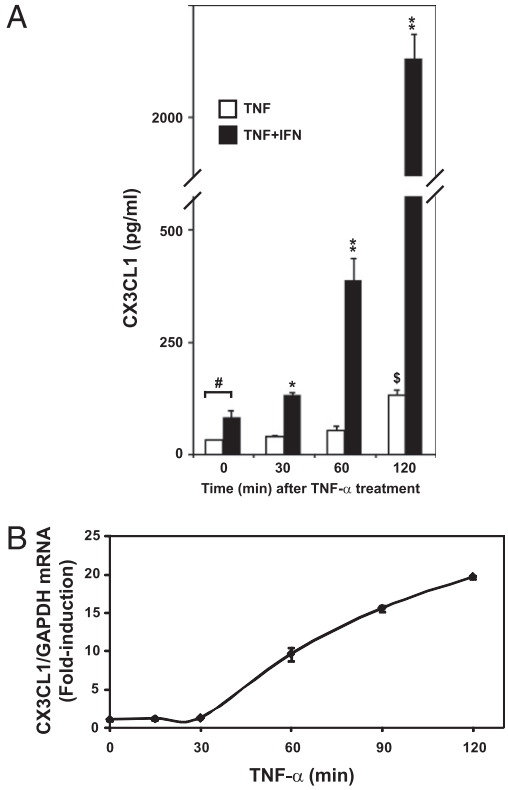

FIGURE 1. TNF-α enhances IFN-γ–induced CX3CL1 production in HUVECs. *A*, The cells were treated with IFN-γ (2 ng/ml) for 16 h, followed by TNF-α (2 ng/ml) for up to 2 h. CX3CL1 production of the cells treated with TNF-α alone (open bar) and those treated with TNF-α after 16 h treatment with IFN-γ (filled bar) was determined by ELISA. Means ± SD from three experiments are shown. $^{\#}p < 0.001$ versus unstimulated cells; $*p < 0.01$; $**p < 0.001$ versus IFN-γ–treated, TNF-α–untreated cells (TNF + IFN 0 min); $^{\$}p < 0.001$ versus unstimulated cells. *B*, Time course of CX3CL1 mRNA expression in HUVECs stimulated with TNF-α (2 ng/ml). The levels of mRNA were determined by quantitative RT-PCR as described in *Materials and Methods*. GAPDH served as a normalization control. The data plotted represent the average of three determinations.

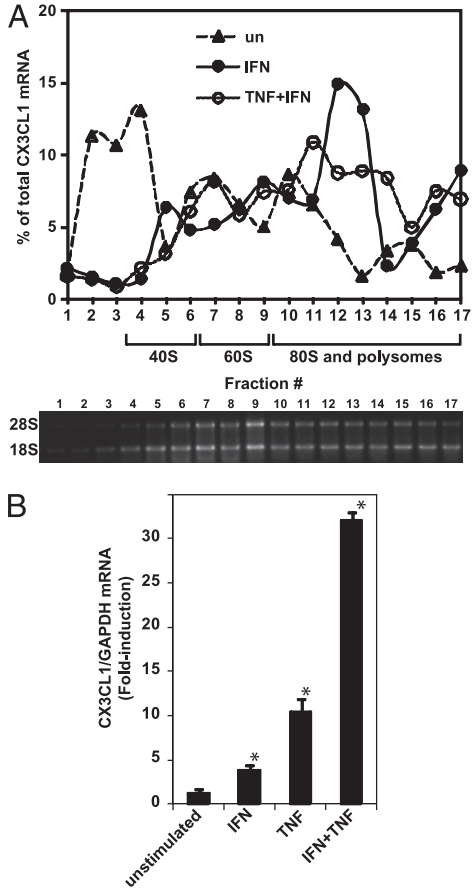

FIGURE 2. CX3CL1 polysome profile in HUVECs. *A*, Cytoplasmic fractions from lysates of the cells exposed to IFN-γ (2 ng/ml) for 16 h and IFN-γ for 16 h, followed by TNF-α treatment (2 ng/ml) for 1 h. Unstimulated controls were subjected to centrifugation on a continuous 15–50% sucrose gradient. Polysome profiles were obtained by running RNA samples from each fraction on an agarose gel electrophoresis to identify the 40S, 60S, and 80S ribosomal subunits and polysomes (*bottom panel*). The distribution of CX3CL1 mRNA from the cells treated with IFN-γ (filled circles), the cells treated with IFN-γ followed by TNF-α (open circles), and unstimulated control cells (filled triangles) was analyzed by RT-PCR of gradient fractions. *B*, Cells were treated with IFN-γ for 16 h followed by TNF-α for 1 h. The levels of mRNA were determined by quantitative RT-PCR. The data plotted represent the average of three determinations. $*p < 0.01$, versus unstimulated cells.

Transfection

Transient transfections of A549 cells were accomplished by plating cells at a density of 1.5×10^5 cells per well of a 24-well culture plate 18–20 h before transfection. Three hundred nanograms of full-length CX3CL1 3′UTR or its mutants and 50 ng pSV-β-Gal (Promega) were cotransfected using 1.5 μl of an Attractene transfection reagent (Qiagen) following the vendor's instructions. The cells were incubated for 24 h and then analyzed for the reporter activity. For the mRNA decay analysis, A549 cells, grown 70–80% of confluence in a 35-mm dish, were cotransfected with the 500 ng of the pcDNA-Luc vectors and 100 ng pCMV-HA expression vector or pCMV-HA–HuR, using 4.5 μl Attractene. The cells were incubated for 24 h and then analyzed for the expression of luciferase mRNA.

Reporter assay

Twenty-four hours after the transfection, the cells were harvested in Reporter lysis buffer (Progema), and the luciferase activity was determined by Luciferase assay system (Progema). Luciferase activities were normalized by transfection efficiency by β-galactosidase activity measured using a β-galactosidase reporter gene assay chemiluminescence kit (Roche, Basel, Switzerland). Data were presented as mean ± SD of at least three independent experiments done in duplicate.

Immunoblot analyses

The cells were washed twice with PBS and lysed in NRSB-minus buffer (62.5 mM Tris [pH 6.8], 1 mM sodium vanadate, 1 mM sodium fluoride, 2% SDS, and 10% glycerol). After sonication, the lysate was cleared by centrifugation at $12{,}000 \times g$ for 10 min at 15°C. The cell lysate (15 μg protein) was subjected to electrophoresis on a 12% SDS-PAGE gel, and the proteins were transferred to a polyvinylidene difluoride membrane (Millipore, Billerica, MA) that was then blocked for 60 min at room temperature in 1× TBST buffer (50 mM Tris-HCl [pH 7.5], 250 mM NaCl, 0.1% Tween 20) containing either 5% nonfat dry milk or 5% BSA. The membrane was incubated at 4°C overnight with one of the following primary Abs: rabbit monoclonal anti-phospho–p38 MAPK (Thr180/Tyr182), rabbit polyclonal anti-p38 MAPK, rabbit monoclonal anti-phospho–MAPK-activated protein kinase (MAPKAPK)-2 (Thr334), rabbit polyclonal anti–MAPKAPK-2 (Cell Signaling Technology, Beverly, MA), and rabbit polyclonal anti-actin (Sigma-Aldrich). After five washes with blocking solution, the membrane was incubated for 1 h at room temperature with HRP-conjugated bovine anti-rabbit IgG or anti-mouse IgG (1:5000; Santa Cruz Biotechnology, Santa Cruz, CA). The immunoreactive bands were visualized using chemiluminescence detection reagents (Pierce, Rockford, IL).

Immunofluorescence staining for HuR

HUVECs grown on a gelatin-coated glass coverslip were rinsed in PBS, fixed with 4% formaldehyde in PBS (20 min), permeabilized with 0.1% Triton X-100 in PBS (10 min), and blocked by incubating with 5% BSA in PBS for 1 h. The cells were then incubated for 1 h with a mouse monoclonal anti-HuR Ab (1:100) or control-mouse IgG (Santa Cruz Biotechnology). After washing, the cells were incubated with Alexa 594-conjugated anti-mouse IgG (Molecular Probes, Eugene, OR). Excess reagents were washed with PBS, and stained

cells were incubated in mounting media containing DAPI (Vectashield, Burlingame, CA). Intracellular localization of HuR was examined under an Olympus BX60 epifluorescence microscope, and the relative distribution between the nucleus and cytoplasm was quantitatively assessed.

Isolation of endogenous CX3CL1 mRNA-HuR complex

Isolation of the mRNA-protein complex was performed as previously reported by Tenebraum et al. (27) with slight modification. HUVECs grown in a 60-mm dish were washed twice with ice-cold PBS and harvested in 500 μl polysome lysis buffer (100 mM KCl, 5 mM $MgCl_2$, 10 mM HEPES [pH7.5], 0.5% NP-40, 1 mM DTT) containing RNase Out (100 U/ml) and 0.2% protease inhibitor mixture. The lysate was allowed to sit on ice for 10 min. After the homogenization with 15 strokes of a tight Dounce homogenizer, the lysate was centrifuged twice at 12,000 × *g* for 10 min at 4°C, and the Sup was collected. Protein A/G-agarose plus (Santa Cruz Biotechnology) was blocked in NT2 buffer (50 mM Tris [pH 7.4], 150 mM NaCl, 1 mM $MgCl_2$, 0.05% NP-40) supplemented with 5% BSA for 1 h at 4°C with gentle agitation and then coated with 10 μl anti-HuR mouse mAb (Santa Cruz Biotechnology) or a normal mouse IgG (Santa Cruz Biotechnology) for 1 h at 4°C with gentle agitation. Immunoprecipitaion was accomplished by adding the following mixture to the Ab-coated beads: 850 μl NT2 Buffer, 100 U/m RNase Out, 10 mM DTT, 20 mM EDTA, and 100 μl HUVEC homogenate Sup. Two hours after the immunoprecipitation reaction at 4°C with gentle agitation, the reaction mixture was centrifuged at 700 × *g* for 1 min, and the Sup was collected. Next, the beads were extensively washed with NT2 buffer. After the final wash, the beads were resuspended in buffer RLT, lysis buffer for RNA supplied in the RNeasy kit, and RNAs from the collected Sup sample and the sample eluted from the beads (immunoprecipitated) were extracted using an RNeasy kit. RT-PCR for CX3CL1 and GAPDH were performed, and the amplified products were analyzed by electrophoresis on a 1.5% agarose gel.

Results

TNF-α stimulates IFN-γ–induced CX3CL1 production in HUVECs

The cytokine-induced CX3CL1 production in HUVECs is summarized in Fig. 1. IFN-γ clearly increased CX3CL1 production in HUVECs (Fig. 1*A*). TNF-α also stimulated CX3CL1 production in a time-dependent manner, and the effect was observed after 2 h of the stimulation (Fig. 1*A*). When the cells were treated with TNF-α 16 h after treatment with IFN-γ, CX3CL1 production was robustly increased, and the effect was observed as early as 30 min after stimulation with TNF-α (Fig. 1*A*). The level of CX3CL1 mRNA in HUVECs was upregulated after 60 min of the stimulation with TNF-α (Fig. 1*B*).

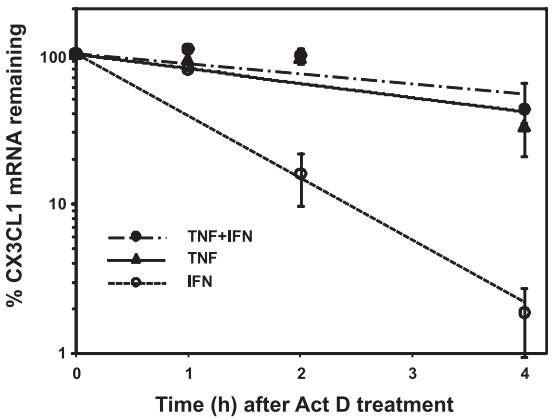

FIGURE 3. Stabilization of CX3CL1 mRNA by TNF-α. Decay of CX3CL1 mRNA was determined in the cells treated with Act D by quantitative RT-PCR. Act D (5 μg/ml) was added after the treatment with TNF-α for 1 h (filled triangles), IFN-γ for 16 h (open circles), and IFN-γ for 16 h followed by TNF-α for 1 h (filled circles). Data are mean ± SD of three experiments.

Polysomal distribution of CX3CL1 mRNA in HUVECs stimulated with IFN-γ and TNF-α

Fig. 2*A* shows the result of the polysome profile analysis on the translational status of CX3CL1 mRNA in HUVECs. Most of the CX3CL1 transcripts from unstimulated cells were associated with ribosome-free fractions. The IFN-γ–induced CX3CL1 transcripts were found to be associated with monosomal fractions, and there was also a large peak in 80S ribosomal fraction followed by polyribosomal fractions. Basically, TNF-α did not alter the polysomal distribution in response to IFN-γ; however, the quantitative analysis revealed that the level of CX3CL1 mRNA was

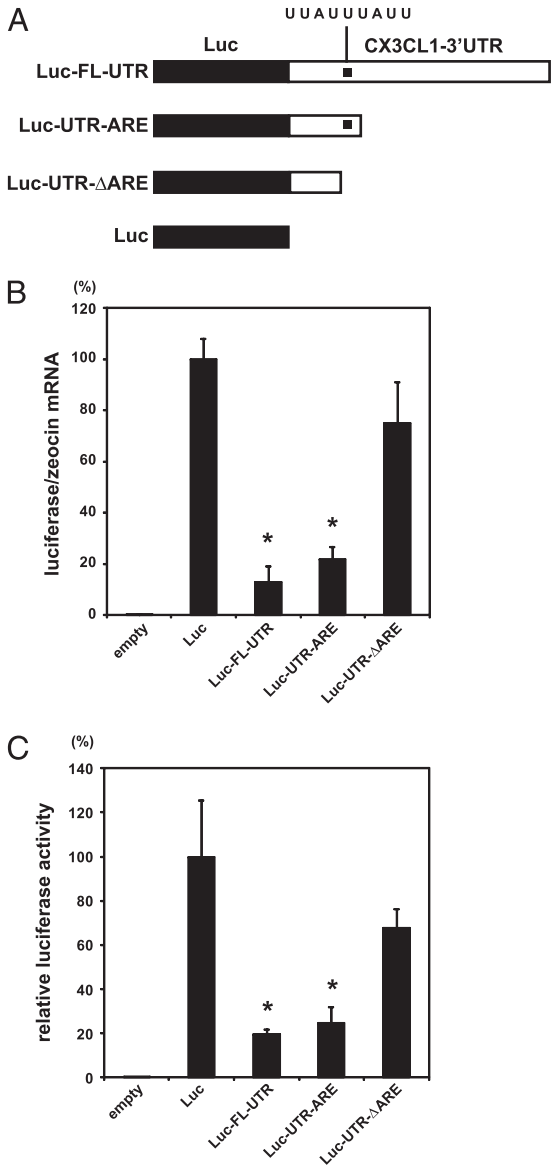

FIGURE 4. The 3′UTR-mediated destabilization of CX3CL1 mRNA. *A*, A series of various deletions of the 2014-nucleotide CX3CL1 3′UTR (open bars) were fused to luciferase reporter gene (black bars) to create an expression construct containing the luciferase cDNA fused to the full-length CX3CL1 3′UTR (Luc-FL-UTR), the putative CX3CL1 AU-rich element (Luc-UTR-ARE), the 3′UTR deleted AU-rich element (Luc-UTR-ΔARE), or luciferase without a 3′UTR (Luc). The *filled square* represents AU-rich nonamer, UUAUUUAUU, contained within the 3′UTR. A549 cells were transfected with one of the Luc-fused vectors. *B*, mRNA level was determined using quantitative RT-PCR. *C*, Luciferase production was assessed by measuring the luciferase activity. Result represents the mean ± SD of three separate transfection experiments. $*p < 0.01$ versus Luc.

boosted by briefly exposing IFN-γ–treated HUVECs to TNF-α (Fig. 2*B*).

TNF-α stabilizes IFN-γ–induced CX3CL1 mRNA

The results on the half-life of CX3CL1 mRNA, in the presence of actinomycin D (Act D), are shown in Fig. 3. After Act D treatment, the decay of CX3CL1 mRNA in the TNF-α–treated cells was relatively slow. In contrast, the decay in the IFN-γ–treated cells was significantly faster as compared with the cells stimulated with TNF-α. The decay of CX3CL1 mRNA in the IFN-γ–treated cells was rescued by TNF-α: the half-lives of CX3CL1 mRNA in the cells stimulated with TNF-α, IFN-γ, and both TNF-α and IFN-γ were calculated to be ~200, 40, and 240 min, respectively.

Single AU-rich element is sufficient for posttranscriptional regulation of CX3CL1 mRNA

To analyze whether CX3CL1 mRNA is regulated posttranscriptionally, we cloned full-length 3′UTR of CX3CL1 mRNA from HUVECs. The total length of the mRNA 3′UTR was 2014 nt (GenBank accession no. GU047346; www.ncbi.nlm.nih.gov/Genbank/). There was a single UUAUUUAUU nonamer that was located within 298–306 nt from the stop codon in the CX3CL1 3′UTR.

To determine the effect of CX3CL1 3′UTR, expression constructs containing luciferase and the full-length CX3CL1 3′UTR, a highly conserved AU-rich region of the 3′UTR, or a truncated form of the 3′UTR without the AU-rich region were generated (Fig. 4*A*). It is reported that TNF-α and IFN-γ synergistically induce CX3CL1 in both A549 lung cancer cells and HUVECs (15), and A549 cells were used as an experimental model for the transfection study. Fig. 4*B* shows the CX3CL1-3′UTR–dependent luciferase mRNA expression in A549 cells transfected with one of the constructs. Luciferase mRNA was constitutively expressed in the cells transfected with the mammalian expression vector inserted with luciferase cDNA. The addition of full-length CX3CL1 3′UTR to luciferase mRNA significantly lowered the levels of luciferase mRNA. The truncated 3′UTR containing a UUAUUUAUU nonamer still had the suppressive effect on the luciferase mRNA levels; however, deletion of the UUAUUUAUU nonamer from the 3′UTR abolished the suppression on the luciferase mRNA. The results on luciferase protein expression agreed with those on mRNA levels (Fig. 4*C*). When the AU-rich element (ARE) nonamer was mutated or deleted, the luciferase activity was significantly enhanced, compared with the activity with the wild-type ARE (Fig. 5*A*, 5*B*)

Effect of a p38 MAPK inhibitor on the CX3CL1 stabilization

Fig. 5 shows the effect of SB203580, an inhibitor of p38 MAPK, on the cytokine-induced CX3CL1 mRNA stabilization. SB203580 treatment accelerated the decay of CX3CL1 mRNA in HUVECs stimulated with TNF-α (Fig. 6*A*), but it did not alter the decay curve of CX3CL1 mRNA in the cells stimulated with IFN-γ (Fig. 6*B*). SB203580 treatment also accelerated the degradation of CX3CL1 mRNA in HUVECs stimulated with both IFN-γ and TNF-α (Fig. 6*C*).

Fig. 7 shows the effects of SB203580 on luciferase expression in A549 cells transfected with the luciferase cDNA fused with full-length 3′UTR of CX3CL1 (Fig. 4*A*). TNF-α significantly enhanced the luciferase activity in the cells, whereas IFN-γ did not. Costimulation with TNF-α and IFN-γ also increased the luciferase activity, and the pretreatment of the cells with SB203580 significantly inhibited the luciferase activity enhanced by TNF-α alone or both IFN-γ and TNF-α (Fig. 7).

Effects of TNF-α on activation of MAPKAPK-2 and translocation of RNA-stabilizing protein HuR

In HUVECs, TNF-α stimulated phosphorylation of p38 MAPK and its immediate downstream molecule MAPKAPK-2, whereas IFN-γ had no such effect (Fig. 8*A*). The subcellular localization of HuR, an mRNA stabilizer, in HUVECs is shown in Fig. 8*B*. Fig. 8*C* shows the changes in the HuR localization in response to IFN-γ or TNF-α. In unstimulated cells, HuR localized virtually exclusively in the nucleus (96.4 ± 2.7%), and IFN-γ did not alter the subcellular distribution (95.7 ± 2.8% in the nucleus). When the cells were treated with TNF-α, ~12% of HuR was detected in cytoplasm (nuclear HuR, 87.0 ± 4.5%). Treatment of the cells with IFN-γ followed by TNF-α led to marked shift of HuR into the cytoplasm (cytoplasmic HuR, 30.2 ± 4.2%; nuclear HuR, 69.8 ± 4.2%).

Fig. 9 summarizes the effect of SB203580, a p38 MAPK inhibitor, on the TNF-α–induced phosphorylation of MAPKAPK-2 in HUVECs. Pretreatment with SB203580 inhibited the TNF-α–induced phosphorylation of MAPKAPK-2 as shown in Fig. 9*A*.

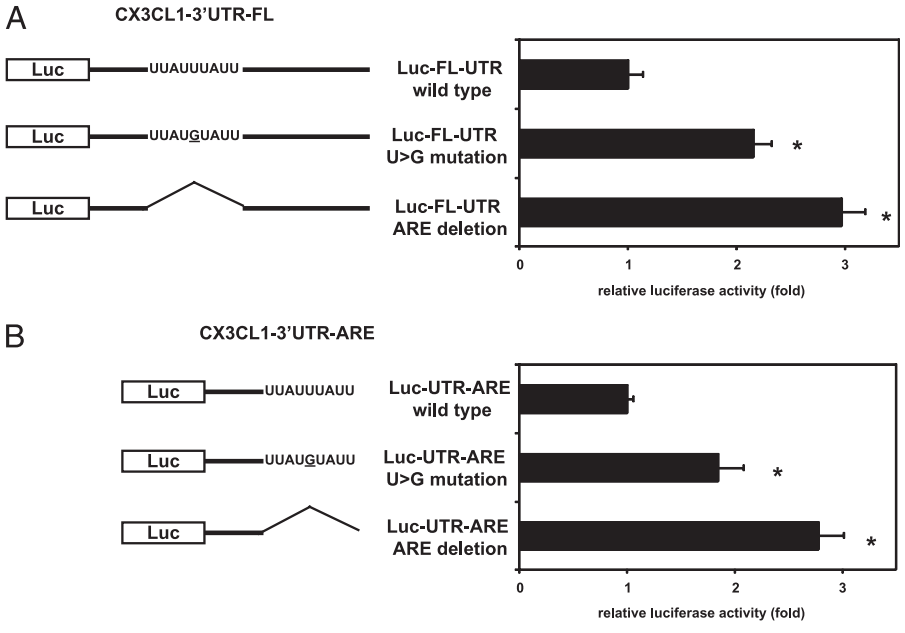

FIGURE 5. The role of ARE in CX3CL1 mRNA instability. *Left schemata* show wild type, U > G point mutated (U > G mutation) and UUAUUUAUU nonamer deleted (ARE deletion) ARE of Luc-FL-UTR (*A*) or Luc-UTR-ARE (*B*), respectively (see Fig. 4*A* for Luc-based constructs). After the transfection of A549 cells with one of the constructs, the levels of luciferase production were assessed by measuring the luciferase activity. Result represents mean ± SD of three separate transfection experiments. $*p < 0.01$ versus wild type.

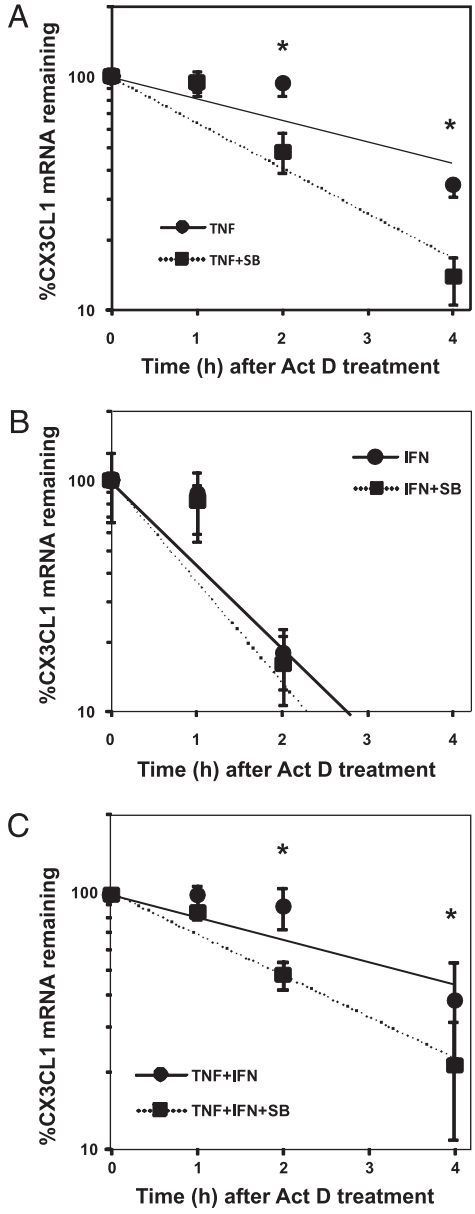

FIGURE 6. Effect of p38 MAPK inhibitor SB203580 on CX3CL1 mRNA instability. HUVECs were treated with TNF-α for 1 h (*A*), IFN-γ for 16 h (*B*), or IFN-γ for 16 h followed by TNF-α for 1h (*C*). Act D (5 μg/ml) with control vehicle (filled circles) or SB203580 (1 μM, filled squares) were then added. Decay of CX3CL1 mRNA was determined using quantitative RT-PCR. Data are means ± SD of three experiments. $*p < 0.01$ versus control vehicle.

SB203580 pretreatment also abolished cytoplasmic HuR protein, which was induced by TNF-α (Fig. 9*B*).

HuR coprecipitates with CX3CL1 mRNA

Results of immunoprecipitation for the mRNA-protein complex with CX3CL1 mRNA and HuR protein are shown in Fig. 10*A*. When endogenous HuR was immunoprecipitated from the cytoplasmic fraction of TNF-α–stimulated HUVECs, the protein was coprecipitated with CX3CL1 mRNA. No PCR product was detected in the sample immunoprecipitated with nonimmune IgG.

ARE is required for the stabilization of CX3CL1 mRNA by HuR

Fig. 10*B* summarizes the results on the decay of CX3CL1 mRNA in A549 cells transfected with one of the chimeric luciferase-CX3CL1 3′UTR fusion constructs (Fig. 4*A*) with or without HuR cDNA.

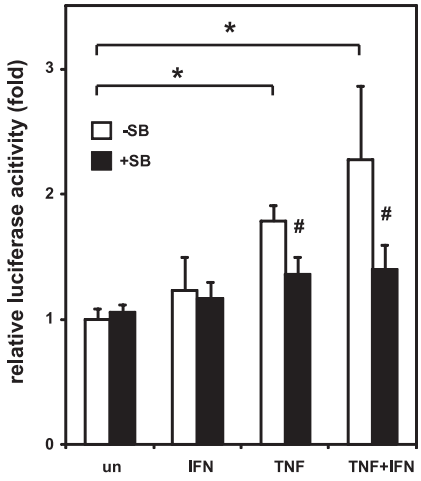

FIGURE 7. Effect of SB203580 on 3′UTR-dependent instability of CX3CL1. A549 cells were transfected with cDNA fused to the full-length CX3CL1 3′UTR. After the transfection, the cells were pretreated with control vehicle (open bars) or SB203580 (1 μM, filled bars) for 30 min, followed by the 16 h stimulation with IFN-γ, TNF-α, or TNF-α and IFN-γ. The levels of luciferase production were assessed by measuring the luciferase activity. Result represents the mean ± SD of three separate transfections. $**p < 0.001$ versus unstimulated control; $^{\#}p < 0.01$ versus vehicle control.

When these cells were treated with Act D, no decay was observed in the cells transfected with control luciferase mRNA. The full-length 3′UTR (Luc-FL-UTR) and the conserved ARE of the 3′UTR (Luc-UTR-ARE) gave instability on the reporter luciferase mRNA, whereas the removal of the ARE (Luc-UTR-ΔARE) resulted in the stabilization of mRNA. Cotransfection of the cells with HuR cDNA significantly enhanced mRNA stability of Luc-FL-UTR and Luc-UTR-ARE, both of which contained ARE; however, overexpression of HuR did not affect the stability of mRNA for control luciferase or Luc-UTR-ΔARE, which lacked ARE.

Discussion

In the current study, the role of the posttranscriptional gene regulation was defined in the synergistic induction of CX3CL1 mRNA in response to TNF-α and IFN-γ. Previous studies concluded that the coordinate effect of TNF-α and IFN-γ on the CX3CL1 expression is due to transcriptional regulation in which these cytokines synergistically stimulate the promoter activity of CX3CL1 (11–14). Costimulation with TNF-α and IFN-γ is known to increase the CX3CL1levels more than 10-fold in astrocytes (12), leading us to speculate the existence of another mechanism, most likely posttranscriptional regulation, involved in the synergism between TNF-α and IFN-γ. The rationale for our hypothesis is that all of the previous reports showed that the synergistic induction of CX3CL1 needs relatively a longer period of stimulation (>4 h) (12–15). Therefore, we speculated that the posttranscriptional effect would be masked by the transcriptional activation by TNF-α itself. Although the TNF-α–induced expression of CX3CL1 mRNA in HUVECs was observed as early as 1 h after stimulation, the increase in CX3CL1 protein levels required at least 2 h. These data are consistent with the previous reports on aortic smooth muscle cells (28), astrocytes (12), and mesangial cells (29). In the current study, CX3CL1 protein was robustly induced when the cells were treated subsequently with IFN-γ and TNF-α, and this "superinduction" was observed on the TNF-α stimulation after 60 min of the IFN-γ treatment. Based on these initial results, we considered that CX3CL1 expression in HUVECs

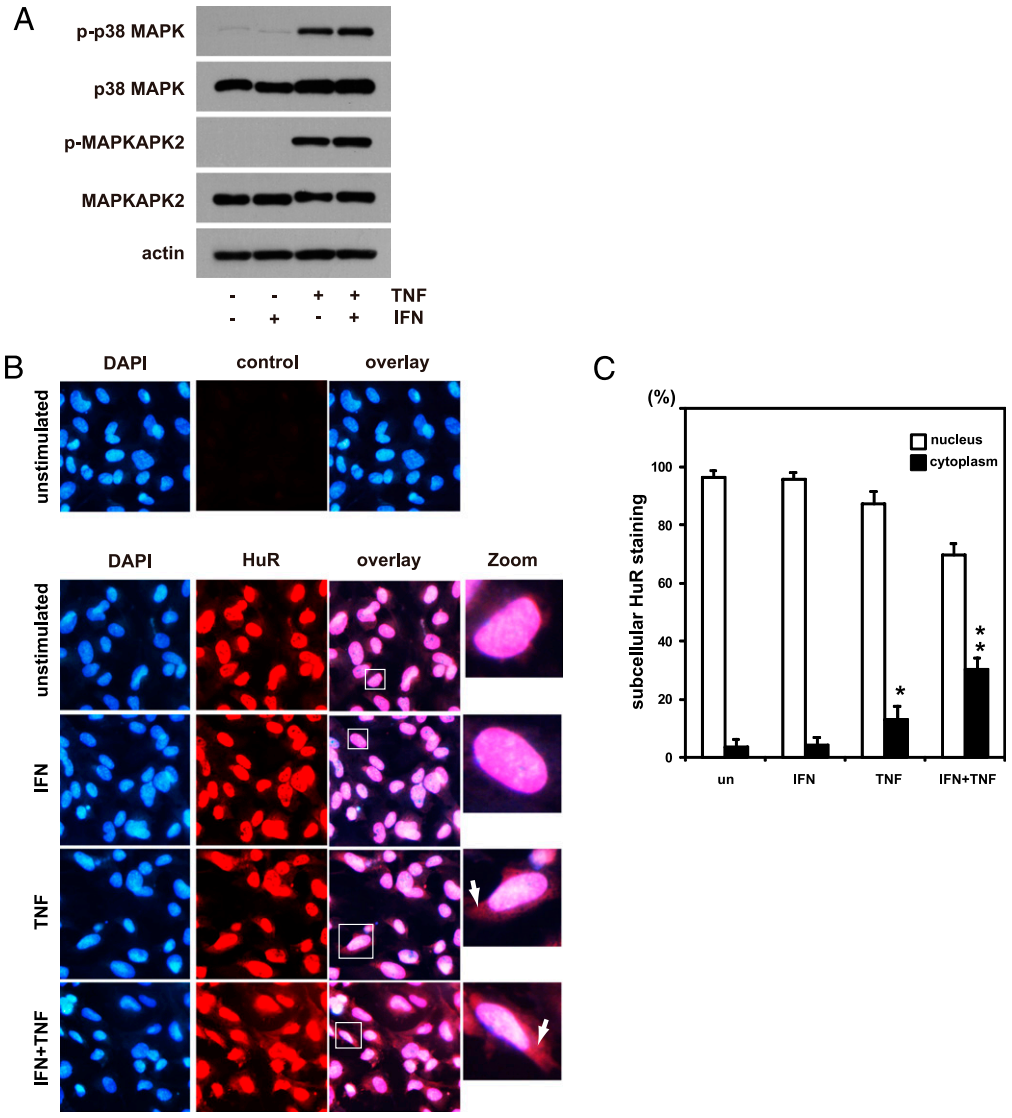

FIGURE 8. Phosphorylation of p38 MAPK and MAPKAPK-2 and cytoplasmic translocation of HuR. HUVECs were treated with IFN-γ for 16 h, TNF-α for 1 h, or IFN-γ for 16 h followed by TNF-α for 1h. *A*, The levels of phosphorylated (p-p38MAPK), total (p38 MAPK) p38 MAPK, phosphorylated MAPKAPK-2 (p–MAPKAPK-2), total MAPKAPK-2 (MAPKAPK-2), and actin were determined by immunoblot analyses as described in *Materials and Methods*. *B*, After the stimulation, the cells were fixed and then incubated with an anti-HuR Ab or mouse nonimmune IgG (control). HuR protein was detected with a secondary Ab coupled Alexa 594 (red). DAPI was used for nuclear definition. Individual images were overlaid. *Zoom* shows an enlargement of a single cell of the merged image. White arrows indicate cytoplasmic HuR staining. Original magnification ×200 (except *Zoom*). *C*, Quantitative analysis on HuR signals from the cytoplasm or nucleus. Five random fields were chosen through the microscope, and fluorescent signals were assessed in 200 cells for each sample. Data shown represent the means from two independent experiments each with three measurements. $*p < 0.05$; $**p < 0.01$ versus control vehicle.

is likely to be regulated by the posttranscriptional and transcriptional mechanisms.

Protein synthesis takes place in a multiple ribosomal structure known as polysome (polyribosome) (30). There are at least two distinct pathways that regulate protein synthesis. One mechanism is the regulation by the assembly or disassembly of polysomes (31). In either Cap-dependent or -independent translation, ribosomal complex tightly proceeds the intricate steps including translational initiation, scanning mRNA and protein elongation. In an inactive state of translation, ribosomes dissociate from mRNA and polyribosomal complexes are disassembled (32), resulting in lighter polysomal or monosomal peaks in polysome profiling assay. The other mechanism that regulates the amount of mRNA in polysomes appears to be fundamentally different (32) (i.e., translation depends on the levels of its template mRNA), which is under the posttranscriptional gene regulation (33), and no alternation in the polysomal distribution is observed. In the current study, IFN-γ was found to shift the polysomal distribution of CX3CL1 mRNA toward polyribosomal fraction, showing that the transcripts were in active translational state; however, TNF-α did not alter the polysomal distribution. A brief exposure to TNF-α, of the cells stimulated with IFN-γ, led to a marked increase in the level of CX3CL1 mRNA. These findings suggest that TNF-α does not alter translational efficiency of a CX3CL1 mRNA template, but does increase the amount of CX3CL1 mRNA in the cells costimulated with IFN-γ. Stabilization of mRNA is the most common type of posttranscriptional regulation (34), and as expected, TNF-α did stabilize the IFN-γ–induced CX3CL1 mRNA.

Several lines of evidence indicate that 3′UTR of mRNA is crucial for both stability and decay of mRNA (34–36). We identified a single AU-rich, perfectly matched, UUAUUUAUU nonamer within the 3′UTR of CX3CL1 mRNA. According to ARE classification, 3′UTR of CX3CL1 is categorized as a class I ARE, which are characterized by the presence of one to three pentamers

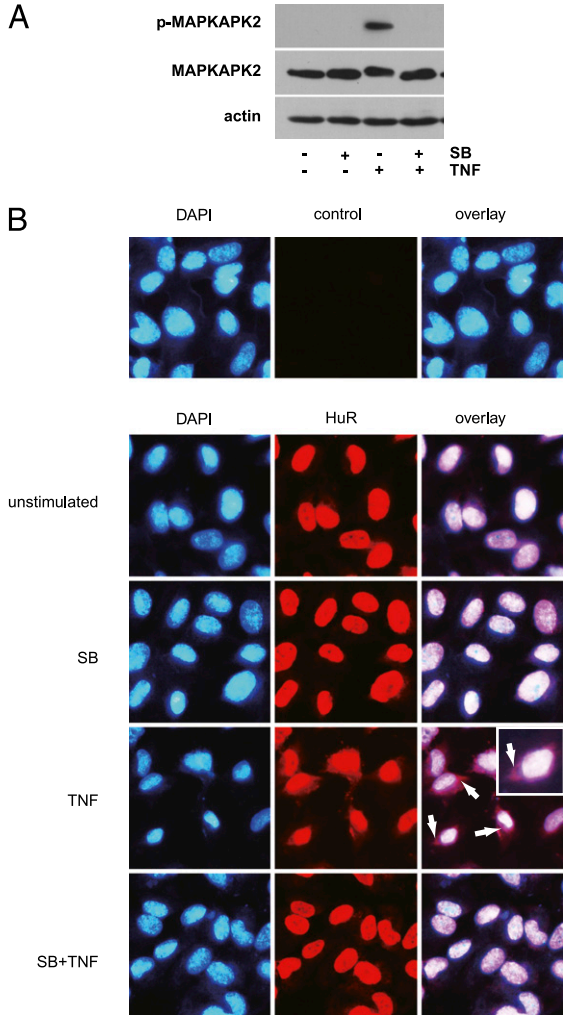

FIGURE 9. Effect of SB203580 on cytoplasmic translocation of HuR. HUVECs were pretreated with control vehicle or SB203580 (1 μM) for 45 min, followed by TNF-α treatment for 30 min (*A*) or 2 h (*B*). *A*, The levels of phosphorylated and total MAPKAPK-2, and actin were determined by immunoblot analyses. *B*, Indirect immunofluorescence against HuR was performed as described in Fig. 8*B*. Original magnification ×200.

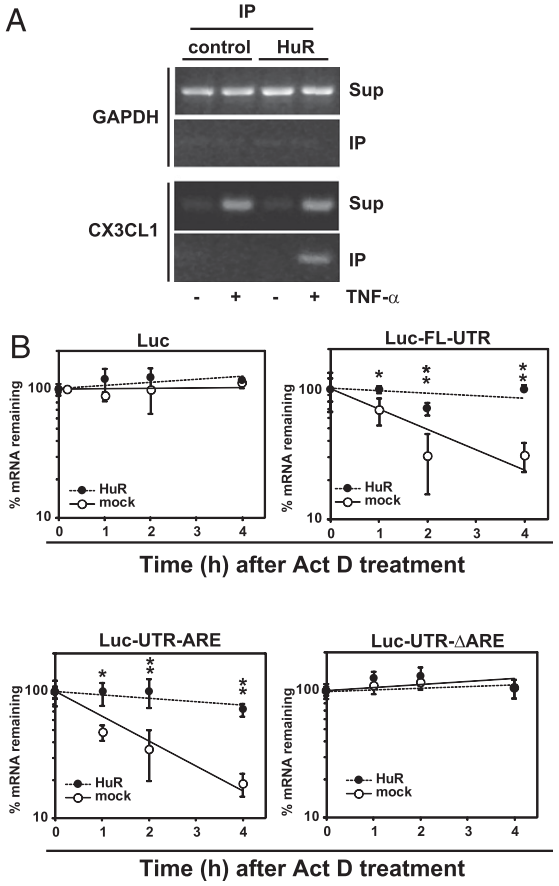

FIGURE 10. Association of HuR with CX3CL1 mRNA. *A*, HuR was immunoprecipitated from cytoplasmic extract of HUVECs treated for TNF-α for 1 h. The mRNAs in the HuR immunocomplex (IP) or supernatant (Sup) were extracted and RT-PCR for CX3CL1 and GAPDH was performed. The PCR products were analyzed by electrophoresis on a 1.5% agarose gel. *B*, HuR requires ARE in the 3′UTR for the stabilization of CX3CL1 mRNA. A549 cells were transfected with Luc, Luc-FL-UTR, Luc-UTR-ARE or Luc-UTR-ΔUTR with HuR cDNA. After the transfection, Act D (5 μg/ml) was added and decay of luciferase mRNA was determined by quantitative RT-PCR. Data are means ± SD of three experiments. $*p < 0.01$; $**p < 0.001$ versus control vehicle. IP, immunoprecipitated.

that are distributed within a large part of the 3′UTR, coupled with a nearby U-rich region (37). Because no other characteristic *cis*-element was found within the 3′UTR, the nonamer was examined for its role in the destabilization of CX3CL1 mRNA. Many observations demonstrated that mRNAs of proto-oncogenes and cytokines are rapidly degraded through the mechanism mediated by AREs (34). The TNF-α–induced expression of CX3CL1 mRNA is also controlled by the accelerated degradation dependent on ARE, and this explains the results of increased CX3CL1 expression in the cells transfected with the nonamer deletion or mutation constructs.

A number of observations suggest the major role of p38 MAPK in the posttranscriptional regulation of proinflammatory genes mediated through ARE in their 3′UTR (38). In addition, TNF-α is known as a potent activator of p38 MAPK (39). Treatment of the cells with p38 MAPK inhibitor SB203580 (40) completely abolished the stabilization of CX3CL1 mRNA induced by TNF-α. Moreover, SB203580 inhibited the TNF-α–increased luciferase activity in the cells introduced the fusion construct of luciferase mRNA and full-length CX3CL1 3′UTR. Thus, the signaling through p38 MAPK might mediate the TNF-α–induced stabilization of CX3CL1 mRNA. MAPKAPK-2, an immediate downstream substrate of p38 MAPK, is known to be a crucial molecule in mRNA stabilization (41, 42). In the current study, IFN-γ did not induce phosphorylation of MAPKAPK-2 as well as that of p38 MAPK in HUVECs. Moreover, IFN-γ did not alter phosphorylation of MAKPAK-2 and p38 MAPK induced by TNF-α. Therefore, TNF-α may be solely responsible for the mRNA stabilization, mediated by the p38 MAPK pathway, resulting in the synergistic induction of CX3CL1 by TNF-α and IFN-γ.

HuR, a member of the embryonic lethal abnormal vision-like family of RNA binding proteins, is known to be one of the most important mRNA stabilizing proteins (43). Molecular mechanism of mRNA stabilization by HuR is still incompletely understood; however, many observations indicate the direct interaction of HuR with ARE-containing mRNA (44). HuR is located in the nucleus under resting conditions and is shuttled from the nucleus to the cytoplasm in response to various cellular stresses (45). This translocation is mediated by the activation of p38 MAPK–MAPKAPK-2 pathway (41, 46, 47). Our data also confirmed that p38 MAPK mediates the TNF-α–mediated cytoplasmic translocation of HuR in HUVECs. Furthermore, pretreatment of the cells with IFN-γ markedly enhanced the TNF-α–induced cytoplasmic translocation of HuR. IFN-γ is known to induce a variety of genes

including cytokines and some of them are synergistically induced by IFN-γ and TNF-α (15, 21, 22) or by IFN-γ and LPS (48). mRNAs of many cytokines have ARE in their 3′UTR (49). Thus, in HUVECs the IFN-γ–induced expression of such ARE-containing cytokines, including CX3CL1, may be short-lived because HuR may not protect their mRNA. However, marked increase in cytoplasmic HuR by combined treatment with IFN-γ and TNF-α may lead to the protection of CX3CL1 mRNA by HuR, which is induced and shuttled to cytoplasm through the activation of p38 MAPK. These results are consistent with that of the immunoprecipitation experiment. In the immunoprecipitation experiment using the cytoplasmic fraction of HUVECs stimulated with TNF-α, HuR was found to coprecipitate with CX3CL1 mRNA. HuR was also confirmed to stabilize CX3CL1 mRNA in the cells transfected with the full-length 3′UTR of CX3CL1; however, the mRNA stabilization was not observed in the cells transfected with the construct lacking ARE.

In conclusion, CX3CL1 expression is regulated by the post-transcriptional mechanism, which involves the stabilization of CX3CL1 mRNA mediated by the p38 MAPK–MAPKAPK-2 activation, followed by shuttling of HuR to the cytoplasm and the binding of HuR to the ARE in 3′UTR. TNF-α utilizes these mechanisms in the synergistic induction of CX3CL1 with IFN-γ. Because TNF-α and IFN-γ are considered potential key molecules in atherosclerosis (2), the posttranscriptional regulation of CX3CL1 in the vascular endothelium may serve as one of the important molecular processes precipitating atherosclerosis.

Acknowledgments

We thank Dr. Stephen M. Prescott of the Oklahoma Medical Research Foundation for helpful discussions and Kumiko Munakata, Michiko Nakata, and Miho Ono for technical assistance.

Disclosures

The authors have no financial conflicts of interest.

References

1. Glass, C. K., and J. L. Witztum. 2001. Atherosclerosis. The road ahead. *Cell* 104: 503–516.
2. Young, J. L., P. Libby, and U. Schönbeck. 2002. Cytokines in the pathogenesis of atherosclerosis. *Thromb. Haemost.* 88: 554–567.
3. Harvey, E. J., and D. P. Ramji. 2005. Interferon-γ and atherosclerosis: pro- or anti-atherogenic? *Cardiovasc. Res.* 67: 11–20.
4. Kleemann, R., S. Zadelaar, and T. Kooistra. 2008. Cytokines and atherosclerosis: a comprehensive review of studies in mice. *Cardiovasc. Res.* 79: 360–376.
5. Pennica, D., G. E. Nedwin, J. S. Hayflick, P. H. Seeburg, R. Derynck, M. A. Palladino, W. J. Kohr, B. B. Aggarwal, and D. V. Goeddel. 1984. Human tumour necrosis factor: precursor structure, expression and homology to lymphotoxin. *Nature* 312: 724–729.
6. Schroder, K., P. J. Hertzog, T. Ravasi, and D. A. Hume. 2004. Interferon-gamma: an overview of signals, mechanisms and functions. *J. Leukoc. Biol.* 75: 163–189.
7. Lusis, A. J. 2000. Atherosclerosis. *Nature* 407: 233–241.
8. Paludan, S. R. 2000. Synergistic action of pro-inflammatory agents: cellular and molecular aspects. *J. Leukoc. Biol.* 67: 18–25.
9. Bazan, J. F., K. B. Bacon, G. Hardiman, W. Wang, K. Soo, D. Rossi, D. R. Greaves, A. Zlotnik, and T. J. Schall. 1997. A new class of membrane-bound chemokine with a CX3C motif. *Nature* 385: 640–644.
10. Imai, T., K. Hieshima, C. Haskell, M. Baba, M. Nagira, M. Nishimura, M. Kakizaki, S. Takagi, H. Nomiyama, T. J. Schall, and O. Yoshie. 1997. Identification and molecular characterization of fractalkine receptor CX3CR1, which mediates both leukocyte migration and adhesion. *Cell* 91: 521–530.
11. Teupser, D., S. Pavlides, M. Tan, J. C. Gutierrez-Ramos, R. Kolbeck, and J. L. Breslow. 2004. Major reduction of atherosclerosis in fractalkine (CX3CL1)-deficient mice is at the brachiocephalic artery, not the aortic root. *Proc. Natl. Acad. Sci. USA* 101: 17795–17800.
12. Yoshida, H., T. Imaizumi, K. Fujimoto, N. Matsuo, K. Kimura, X. Cui, T. Matsumiya, K. Tanji, T. Shibata, W. Tamo, et al. 2001. Synergistic stimulation, by tumor necrosis factor-α and interferon-γ, of fractalkine expression in human astrocytes. *Neurosci. Lett.* 303: 132–136.
13. Fraticelli, P., M. Sironi, G. Bianchi, D. D'Ambrosio, C. Albanesi, A. Stoppacciaro, M. Chieppa, P. Allavena, L. Ruco, G. Girolomoni, et al. 2001. Fractalkine (CX3CL1) as an amplification circuit of polarized Th1 responses. *J. Clin. Invest.* 107: 1173–1181.
14. Sukkar, M. B., R. Issa, S. Xie, U. Oltmanns, R. Newton, and K. F. Chung. 2004. Fractalkine/CX3CL1 production by human airway smooth muscle cells: induction by IFN-γ and TNF-α and regulation by TGF-β and corticosteroids. *Am. J. Physiol. Lung Cell. Mol. Physiol.* 287: L1230–L1240.
15. Bhavsar, P. K., M. B. Sukkar, N. Khorasani, K. Y. Lee, and K. F. Chung. 2008. Glucocorticoid suppression of CX3CL1 (fractalkine) by reduced gene promoter recruitment of NF-kappaB. *FASEB J.* 22: 1807–1816.
16. Wong, G. H., and D. V. Goeddel. 1986. Tumour necrosis factors α and β inhibit virus replication and synergize with interferons. *Nature* 323: 819–822.
17. Meyer, R., E. N. Hatada, H. P. Hohmann, M. Haiker, C. Bartsch, U. Röthlisberger, H. W. Lahm, E. J. Schlaeger, A. P. van Loon, and C. Scheidereit. 1991. Cloning of the DNA-binding subunit of human nuclear factor κ B: the level of its mRNA is strongly regulated by phorbol ester or tumor necrosis factor alpha. *Proc. Natl. Acad. Sci. USA* 88: 966–970.
18. Levy, D. E., D. J. Lew, T. Decker, D. S. Kessler, and J. E. Darnell, Jr. 1990. Synergistic interaction between interferon-α and interferon-γ through induced synthesis of one subunit of the transcription factor ISGF3. *EMBO J.* 9: 1105–1111.
19. Ohmori, Y., and T. A. Hamilton. 1995. The interferon-stimulated response element and a κ B site mediate synergistic induction of murine IP-10 gene transcription by IFN-γ and TNF-α. *J. Immunol.* 154: 5235–5244.
20. Qi, X. F., D. H. Kim, Y. S. Yoon, D. Jin, X. Z. Huang, J. H. Li, Y. K. Deung, and K. J. Lee. 2009. Essential involvement of cross-talk between IFN-γ and TNF-α in CXCL10 production in human THP-1 monocytes. *J. Cell. Physiol.* 220: 690–697.
21. Jahnke, A., and J. P. Johnson. 1994. Synergistic activation of intercellular adhesion molecule 1 (ICAM-1) by TNF-α and IFN-γ is mediated by p65/p50 and p65/c-Rel and interferon-responsive factor Stat1 α (p91) that can be activated by both IFN-γ and IFN-α. *FEBS Lett.* 354: 220–226.
22. Imanishi, D., K. Yamamoto, H. Tsushima, Y. Miyazaki, K. Kuriyama, M. Tomonaga, and T. Matsuyama. 2000. Identification of a novel cytokine response element in the human IFN regulatory factor-1 gene promoter. *J. Immunol.* 165: 3907–3916.
23. Winzen, R., M. Kracht, B. Ritter, A. Wilhelm, C. Y. Chen, A. B. Shyu, M. Müller, M. Gaestel, K. Resch, and H. Holtmann. 1999. The p38 MAP kinase pathway signals for cytokine-induced mRNA stabilization via MAP kinase-activated protein kinase 2 and an AU-rich region-targeted mechanism. *EMBO J.* 18: 4969–4980.
24. Imaizumi, T., H. Itaya, K. Fujita, D. Kudoh, S. Kudoh, K. Mori, K. Fujimoto, T. Matsumiya, H. Yoshida, and K. Satoh. 2000. Expression of tumor necrosis factor-alpha in cultured human endothelial cells stimulated with lipopolysaccharide or interleukin-1alpha. *Arterioscler. Thromb. Vasc. Biol.* 20: 410–415.
25. Matsumiya, T., T. Imaizumi, H. Yoshida, K. Satoh, M. K. Topham, and D. M. Stafforini. 2009. The levels of retinoic acid-inducible gene I are regulated by heat shock protein 90-α. *J. Immunol.* 182: 2717–2725.
26. Dixon, D. A., C. D. Kaplan, T. M. McIntyre, G. A. Zimmerman, and S. M. Prescott. 2000. Post-transcriptional control of cyclooxygenase-2 gene expression. The role of the 3′-untranslated region. *J. Biol. Chem.* 275: 11750–11757.
27. Tenenbaum, S. A., P. J. Lager, C. C. Carson, and J. D. Keene. 2002. Ribonomics: identifying mRNA subsets in mRNP complexes using antibodies to RNA-binding proteins and genomic arrays. *Methods* 26: 191–198.
28. Chandrasekar, B., S. Mummidi, R. P. Perla, S. Bysani, N. O. Dulin, F. Liu, and P. C. Melby. 2003. Fractalkine (CX3CL1) stimulated by nuclear factor kappaB (NF-kappaB)-dependent inflammatory signals induces aortic smooth muscle cell proliferation through an autocrine pathway. *Biochem. J.* 373: 547–558.
29. Chen, Y. M., S. L. Lin, C. W. Chen, W. C. Chiang, T. J. Tsai, and B. S. Hsieh. 2003. Tumor necrosis factor-α stimulates fractalkine production by mesangial cells and regulates monocyte transmigration: down-regulation by cAMP. *Kidney Int.* 63: 474–486.
30. Warner, J. R., P. M. Knopf, and A. Rich. 1963. A multiple ribosomal structure in protein synthesis. *Proc. Natl. Acad. Sci. USA* 49: 122–129.
31. Hershey, J. W. 1991. Translational control in mammalian cells. *Annu. Rev. Biochem.* 60: 717–755.
32. Nelson, E. M., and M. M. Winkler. 1987. Regulation of mRNA entry into polysomes. Parameters affecting polysome size and the fraction of mRNA in polysomes. *J. Biol. Chem.* 262: 11501–11506.
33. Tobey, R. A., E. C. Anderson, and D. F. Petersen. 1966. RNA stability and protein synthesis in relation to the division of mammalian cells. *Proc. Natl. Acad. Sci. USA* 56: 1520–1527.
34. Fan, J., N. M. Heller, M. Gorospe, U. Atasoy, and C. Stellato. 2005. The role of post-transcriptional regulation in chemokine gene expression in inflammation and allergy. *Eur. Respir. J.* 26: 933–947.
35. Behm-Ansmant, I., I. Kashima, J. Rehwinkel, J. Saulière, N. Wittkopp, and E. Izaurralde. 2007. mRNA quality control: an ancient machinery recognizes and degrades mRNAs with nonsense codons. *FEBS Lett.* 581: 2845–2853.
36. von Roretz, C., and I. E. Gallouzi. 2008. Decoding ARE-mediated decay: is microRNA part of the equation? *J. Cell Biol.* 181: 189–194.
37. Zhang, T., V. Kruys, G. Huez, and C. Gueydan. 2002. AU-rich element-mediated translational control: complexity and multiple activities of trans-activating factors. *Biochem. Soc. Trans.* 30: 952–958.
38. Dean, J. L., G. Sully, A. R. Clark, and J. Saklatvala. 2004. The involvement of AU-rich element-binding proteins in p38 mitogen-activated protein kinase pathway-mediated mRNA stabilisation. *Cell. Signal.* 16: 1113–1121.
39. Beyaert, R., A. Cuenda, W. Vanden Berghe, S. Plaisance, J. C. Lee, G. Haegeman, P. Cohen, and W. Fiers. 1996. The p38/RK mitogen-activated

protein kinase pathway regulates interleukin-6 synthesis response to tumor necrosis factor. *EMBO J.* 15: 1914–1923.
40. Birkenkamp, K. U., L. M. Tuyt, C. Lummen, A. T. Wierenga, W. Kruijer, and E. Vellenga. 2000. The p38 MAP kinase inhibitor SB203580 enhances nuclear factor-kappa B transcriptional activity by a non-specific effect upon the ERK pathway. *Br. J. Pharmacol.* 131: 99–107.
41. Subbaramaiah, K., T. P. Marmo, D. A. Dixon, and A. J. Dannenberg. 2003. Regulation of cyclooxgenase-2 mRNA stability by taxanes: evidence for involvement of p38, MAPKAPK-2, and HuR. *J. Biol. Chem.* 278: 37637–37647.
42. Tran, H., M. Schilling, C. Wirbelauer, D. Hess, and Y. Nagamine. 2004. Facilitation of mRNA deadenylation and decay by the exosome-bound, DExH protein RHAU. *Mol. Cell* 13: 101–111.
43. Fan, X. C., and J. A. Steitz. 1998. Overexpression of HuR, a nuclear-cytoplasmic shuttling protein, increases the in vivo stability of ARE-containing mRNAs. *EMBO J.* 17: 3448–3460.
44. Brennan, C. M., and J. A. Steitz. 2001. HuR and mRNA stability. *Cell. Mol. Life Sci.* 58: 266–277.
45. Cok, S. J., S. J. Acton, and A. R. Morrison. 2003. The proximal region of the 3′-untranslated region of cyclooxygenase-2 is recognized by a multimeric protein complex containing HuR, TIA-1, TIAR, and the heterogeneous nuclear ribonucleoprotein U. *J. Biol. Chem.* 278: 36157–36162.
46. Tran, H., F. Maurer, and Y. Nagamine. 2003. Stabilization of urokinase and urokinase receptor mRNAs by HuR is linked to its cytoplasmic accumulation induced by activated mitogen-activated protein kinase-activated protein kinase 2. *Mol. Cell. Biol.* 23: 7177–7188.
47. Lasa, M., K. R. Mahtani, A. Finch, G. Brewer, J. Saklatvala, and A. R. Clark. 2000. Regulation of cyclooxygenase 2 mRNA stability by the mitogen-activated protein kinase p38 signaling cascade. *Mol. Cell. Biol.* 20: 4265–4274.
48. Faure, E., L. Thomas, H. Xu, A. Medvedev, O. Equils, and M. Arditi. 2001. Bacterial lipopolysaccharide and IFN-γ induce Toll-like receptor 2 and Toll-like receptor 4 expression in human endothelial cells: role of NF-κ B activation. *J. Immunol.* 166: 2018–2024.
49. McCormick, C., and D. Ganem. 2005. The kaposin B protein of KSHV activates the p38/MK2 pathway and stabilizes cytokine mRNAs. *Science* 307: 739–741.